Spectrochimica Acta Part A 79 (2011) 1634–1641

Contents lists available at ScienceDirect

Spectrochimica Acta Part A: Molecular and Biomolecular Spectroscopy

journal homepage: www.elsevier.com/locate/saa

Synthesis, spectral and catalytic activity of some Manganese(II) bis-benzimidazole diamide complexes

Subash Chandra Mohapatra [a], M.S. Hundal [b], Pavan Mathur [a,*]

[a] Department of Chemistry, University of Delhi, Delhi 110007, India
[b] Guru Nanak Dev University, Amritsar, India

ARTICLE INFO

Article history:
Received 22 October 2010
Received in revised form 10 May 2011
Accepted 16 May 2011

Keywords:
Benzimidazole diamide
Manganese(II)-Diaqua complex
Hydrogen bonding network
Amine oxidation

ABSTRACT

Four Mn(II) complexes bound to a neutral bis-benzimidazole diamide ligand N,N′-bis(2-methyl benzimidazolyl 2,2′-oxy-diethanamide) (GBOA) have been synthesized and characterized. Anionic ligand associated with the complexes varies as Cl^- CH_3COO^-, SCN^- and $ClO_4{}^-$. X-ray structure of one of the complexes $[Mn(GBOA)_2(H_2O)_2]Cl_2{\cdot}4H_2O$ was solved and shows that the Mn(II) ion is hexacoordinate. Two equatorial positions are occupied by benzimidazole imine nitrogen atoms while the other two sites are occupied by amide carbonyl oxygens. The imine nitrogen and carbonyl oxygens are bound to Mn(II) by different arms of the two ligands while axial sites are occupied by two water molecules. Two Cl^- anions are outside the coordination sphere and form an extensive 3D H-bonded network. Axially distorted octahedral geometry is confirmed for all the four complexes by low temperature EPR spectroscopy. Distortion parameter D was found to be similar for $[Mn(GBOA)_2(H_2O)_2]Cl_2{\cdot}4H_2O$ and $[Mn(GBOA)_2(H_2O)_2]{\cdot}(CH_3COO)_2{\cdot}H_2O$. Cyclic voltammograms have been obtained for all the four complexes and $E_{1/2}$ values are dependant on the anionic ligand being in the coordination sphere or outside. $[Mn(GBOA)_2(H_2O)_2]Cl_2{\cdot}4H_2O$ and $[Mn(GBOA)_2(H_2O)_2]{\cdot}(CH_3COO)_2{\cdot}H_2O$ carry out the selective oxidation of N-benzyldimethylamine, and 1-methyl-pyrollidine to their respective carbonyl products with catalytic efficiency of 35–50%.

1. Introduction

Multidentate ligands have the ability to chelate to metal ions in a terminating fashion and thus prevent the formation of polymeric species. However if some sites are left out during the process of chelation these could end up forming intermolecular Hydrogen bonds and facilitate the formation of extended networks. Such Hydrogen bonding networks have gained attention in view of their capability to generate self assembled supramolecular structures [1–4]. The conventional OH···N and NH···O along with π–π stacking interactions have been found to be the most common cementing force for such supramolecular architectures [5–7]. The present study reports the synthesis and spectral studies of four new Mn(II) Complexes. One of the complex $[Mn(GBOA)_2(H_2O)_2]Cl_2{\cdot}4H_2O$ has been structurally characterized, interestingly the anionic ligand Cl^- is found to be outside the coordination sphere, while two water molecules are coordinated. This leads to extensive intermolecular H-bonding interactions leading to the formation of helical sheets and solvent accessible voids. These positively charged sheets are held by extensive Cl···HO and Cl···HN, H-bonding network in the Di-aqua Mn(II) complex bound to a bisbenzimidazolyl diamide ligand; in this context it may be pertinent to recall the role of chloride ions in photosystem II, where it is proposed that Cl^- ions maintain a proton relay network that allows the transport and release of protons during the water oxidation reaction [8]. Low temperature EPR study has been used to obtain the axial distortion parameter D for all the complexes and it is found to be dependant on whether the anionic ligand is within the coordination sphere or outside. $E_{1/2}$ values have been obtained from the respective cyclic voltammograms and they are found to be related to the D parameter found from EPR work, larger the D value less anodic the $E_{1/2}$. $[Mn(GBOA)_2(H_2O)_2]Cl_2{\cdot}4H_2O$ and $[Mn(GBOA)_2(H_2O)_2]{\cdot}(CH_3COO)_2{\cdot}H_2O$ are found to carry out the oxidation of amines to carbonyl products in the presence of tert.butyl hydroperoxide as an external oxidant, and mimics the amine oxidation activity of a Manganese(II) dependant peroxidase sourced from lignin [9].

2. Experimental

2.1. Materials and physical measurements

Glycine benzimidazole dihydrocloride was prepared by following the procedure reported by Cescon and Day [10]. Spectroscopic

---

* Corresponding author. Tel.: +91 1127667725/1381; fax: +91 1127666605.
E-mail address: pavanmat@yahoo.co.in (P. Mathur).

1386-1425/$ – see front matter © 2011 Elsevier B.V. All rights reserved.
doi:10.1016/j.saa.2011.05.024

grade solvents were used for spectral and electrochemical studies and the rest were freshly distilled off before use. All other chemicals were obtained from commercial sources and used as such. Elemental analysis were obtained from USIC, Delhi University, India. NMR spectra were recorded on a 300 MHz Bruker-spin instrument at IIT, Delhi. Electronic spectra were obtained on a Shimadzu UV-VIS-NIR-1601 spectrometer. Infra red spectra were recorded on Perkin-Elmer FTIR-2000 spectrometer as KBr pellets. Cyclic voltammetric studies were performed on BAS CV 50W instrument. The cyclic voltammograms were obtained in a mixed solvent system 2:8 DMSO: Acetonitrile containing 0.1 M TBAP as supporting electrolyte. A three electrode configuration composed of a Pt disk working electrode (3.1 mm^2 area), a Pt wire counter electrode, and a $Ag/AgNO_3$ reference electrode was used for the measurements. All the above measurements were done at the Department of Chemistry, University of Delhi, Delhi, India. X-band solid state EPR spectra of the Mn(II) complexes were recorded at liquid nitrogen temperatures, at the Department of chemistry, IIT Kanpur, India. X-ray data for the complex $[Mn(GBOA)_2(H_2O)_2](Cl)_2 \cdot 4H_2O$ was collected at the Department of Chemistry, IIT, Roorke, India. Mn(II) complexes were subjected to thermo gravimetric analysis on a Shimadzu-TA-60 WS instrument. Well ground samples were taken and heated at rate of 10 °C/min in inert nitrogen atmosphere from room temperature to 600 °C at the Department of Chemistry, University of Delhi, Delhi.

2.2. Synthesis

2.2.1. Preparation of ligand: N,N′-bis(2-methyl benzimidazolyl-2yl)-2,2′ oxy diethanamide (GBOA)

The bis-benzimidazole diamide ligand N,N′-bis(2-methyl benzimidazolyl-2yl)-2,2′-oxydiethan amide (GBOA) was prepared as described before [11].

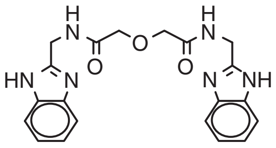

Structural formula of GBOA

2.2.2. Preparation of Mn(II) complexes

A methanolic solution of MnX_2 (0.48 mmol) $\{X = Cl^-, CH_3COO^-, ClO_4^-\}$ was added to the ligand GBOA (0.48 mmol) dissolved in methanol. The solution was stirred for 1 h. The reaction mixture was than concentrated to half of its volume on a water bath. Dropwise addition of a cooled solution of diethyl ether, to the reaction mixture resulted in a white product. This was centrifuged and washed with small amount of acetonitrile and dried over P_2O_5.

2.2.2.1. $[Mn(GBOA)_2(H_2O)_2].(Cl)_2 \cdot 4H_2O(1)$. Yield: 45%, m.p. = 190 °C; CHN:(cal): C:47.1, H:5.1, N:16.5, found: C:47.8, H:4.6, N:16.1; selected IR data (ν/cm^{-1}), 3370 (due to water), 3298, 3100, 1644, 1557, 1449. UV–vis [λ_{max} (nm) (log ε) in MeOH]: 244(4.08), 274(4.12), 282(3.96); $E_{1/2}$ vs Ag/Ag^+: 0.098 V.

2.2.2.2. $[Mn(GBOA)_2(H_2O)_2] \cdot (CH_3COO)_2 \cdot H_2O(2)$. Yield: 50%, m.p. = 230 °C; CHN:(cal): C:52.2, H:5.14, N:16.6, found: C:51.5, H:5.0, N:15.7. Selected IR data (ν/cm^{-1}): 3373 (due to water), 3198, 1664, 1544, 1439, 1419. UV–vis [λ_{max} (nm) (log ε) in MeOH]; 253(3.96), 275(4.02), 281(3.99); $E_{1/2}$ vs Ag/Ag^+: 0.097 V.

2.2.2.3. $[Mn(GBOA)_2(ClO_4)]$ $(ClO_4) \cdot 2CH_3CN(3)$. Yield: 55%, m.p. = 215 °C; CHN:(cal): C:47.1, H:4.1, N:17.5, found: C:48.0, H:5.1, N:16.8. Selected IR data (ν/cm^{-1}): 3280, 1639, 1559, 1450, 1135. UV–vis [λ_{max} (nm) log ε) in MeOH]; 274(3.52), 281(3.50); $E_{1/2}$ vs Ag/Ag^+: 0.058 (V).

2.2.2.4. $[Mn(GBOA)_2(SCN)](SCN) \cdot 4H_2O(4)$. A nearly saturated solution of KSCN in methanol was added dropwise to a methanolic solution of $MnCl_2 \cdot 4H_2O$ (0.48 mmol), until a precipitate started appearing. This solution was centrifuged and the clear centrifugate was added to a methanolic solution of the ligand GBOA (0.48 mmol). Subsequent work up of the reaction was performed as outlined in Section 2.2.1.

Yield: 45%, m.p. = 222 °C, CHN:(cal): C:49.0, H:4.6, N:19.0, S:6.2, found: C:48.0, H:4.5, N:18.0, S:6.2. Selected IR data (ν/cm^{-1}): 3394 (due to water), 3295, 1636, 1543, 1447, 2074. UV–vis [λ_{max} (nm) (log ε) in MeOH]; 270(3.54), 275(3.57), 280(4.18), $E_{1/2}$ vs Ag/Ag^+: 0.080 (V).

2.3. Amine binding and oxidation in presence of tert-butylhydroperoxide

A typical reaction consisted of the following: A 25 ml flask was fitted with a reflux condenser. Manganese complexes $[Mn(GBOA)_2(H_2O)_2] \cdot (Cl)_2 \cdot 4H_2O$ or $[Mn(GBOA)_2(H_2O)_2] \cdot (CH_3COO)_2 \cdot H_2O$ 0.015 mmol and the respective amines (0.3 and 0.15 mmol) in 10 ml CH_3CN were stirred at room temperature for 10 min. Tertiary butyl hydroperoxide (TBHP) [0.02 ml, 0.15 mmol] was then added and reaction mixture stirred for another 15 min. The temperature of the reaction mixture during this period was raised to 50–55 °C degrees and maintained on a water bath. Stirring was continued for $2–2^{1/2}$ h and the reaction was monitored periodically by withdrawing a small volume of the sample and developing a chromatogram in ethyl acetate:hexane (0.5:10). Visualization of the product formed during the course of reaction was carried out by spraying the chromatogram with a solution of 2,4-dinitrophenylhydrazine (DNP). A single spot was observed at $R_f = 0.76–0.79$ cm suggesting the formation of the corresponding carbonyl compound during the course of the above oxidation reaction. The reaction product was isolated by using silica gel column chromatography and respective DNP derivatives were prepared. Benzaldehyde was obtained upon oxidation of N-benzyldimethylamine, while 1-methylpyrollidinone formed from 1-methyl-pyrollidine.

A blank experiment was conducted under identical conditions as reported above in the absence of the Mn(II) complexes and it was found that only 5–7% of the amine was converted to the respective carbonyl product. This therefore confirms the role of the Mn(II) complexes in the oxidation reaction.

Identification of the carbonyl compounds formed was confirmed from ^1H NMR of their respective DNP derivatives:

2.3.1. Benzaldehyde-2-4-DNP-derivative

^1H NMR ($CDCl_3$): δ (ppm) 11.4(s,1H), 9.1(s,1H), 8.41–8.37(d,1H), 8.16–8.11(dd,2H), 8.00–7.97(d,2H), 7.50–7.48(t,3H).

2.3.2. 1-Methyl pyrrolidinone-2-4-DNP-derivative

^1H NMR ($CDCl_3$): δ (ppm) 11.06(s,1H), 9.1(s,1H), 8.32–8.30(d,1H), 8.00–7.96(d,1H), 2.20(t,2H), 2.1(s,3H), 1.26(t,2H), 0.89(q, 2H).

2.4. X-ray crystallography

Crystals of the complex $[Mn(GBOA)_2(H_2O)_2]Cl_2 \cdot 4H_2O$ (**1**) were grown by dissolving the complex synthesized earlier, in methanol and allowing slow diffusion of diethyl ether to this solution in a sealed tube. X-ray data for the complex (**1**) was collected at the Department of Chemistry, IIT, Roorke, India. The data was collected on a Nonius CCD using Mo Kα ($\lambda = 0.71069$). The data was corrected

Table 1
Crystal data and structure refinement for $[Mn(GBOA)_2(H_2O)_2]Cl_2{\cdot}4H_2O$ complex.

Empirical formula	$C_{40}\,H_{52}\,Cl_2\,Mn\,N_{12}\,O_{12}$	
Formula weight	1018.78	
Temperature	293(2) K	
Wavelength	0.71069 Å	
Crystal system	Monoclinic	
Space group	$P2_1/c$	
Unit cell dimensions	$a = 19.992(5)$ Å	$\alpha = 90.000(5)^\circ$
	$b = 10.001(5)$ Å	$\beta = 91.343(5)^\circ$
	$c = 22.971(5)$ Å	$\gamma = 90.000(5)^\circ$
Volume	4592(3) Å^3	
Z	4	
Density (calculated)	1.474 Mg/m^3	
Absorption coefficient	0.479 mm^{-1}	
$F(000)$	2124	
Theta range for data collection	1.02–23.71°	
Index ranges	$-22 \le h \le 22$, $-11 \le k \le 11$, $-25 \le l \le 25$	
Reflections collected	52,992	
Independent reflections	6878 [R(int) = 0.0590]	
Completeness to theta = 23.71°	98.7%	
Absorption correction	None	
Refinement method	Full-matrix least-squares on F^2	
Data/restraints/parameters	6878/0/604	
Goodness-of-fit on F^2	1.026	
Final R indices [$I > 2$ sigma(I)]	R1 = 0.0370, wR2 = 0.0878	
R indices (all data)	R1 = 0.0681, wR2 = 0.1053	
Largest diff. peak and hole	0.327 and −0.281 e Å^{-3}	

for Lorentz and polarization effects. No absorption corrections were applied. The structure was solved by direct methods using SIR-97 [12]. The structure was refined by full-matrix least squares refinement methods based on F^2, using SHELX-97 [13]. Hydrogen atoms were fixed geometrically with their Uiso values 1.2 times their rider atoms. Hydrogens of the water molecules were located from difference Fourier synthesis and were not refined. All calculations were performed using Wingx [14] package. Important crystal and refinement parameters are given in Table 1.

3. Results and discussion

3.1. Electronic spectroscopy, IR data and thermal studies

The electronic spectra of the ligands have two strong bands in the UV region 272–279 nm. These bands are assigned to the π–π^* transition characterizing the benzimidazole group. The spectra of the complexes also show two strong bands in the 273–284 nm corresponding to π–π^* transition, the bands are slightly blue shifted with lowered extinction coefficient.

The free ligand GBOA has characteristics IR bands at 1657 amide **I**($\nu_{C=O}$), 1543 amide **II**($\nu_{C=N}$ amide), 1446 ($\nu_{C=N-C=C}$ benzimidazole). The manganese complexes (**1**–**4**) have amide carbonyl coordination rather than amide **NH**. These bands are in the range of 1664–1636 cm^{-1} (amide I) and 1559–1543 cm^{-1} {amide II} in the Mn(II) complexes [15,16a]. The IR spectra also reveal characteristic stretching frequencies at 1419, 2074, 1135 cm^{-1} assigned for νCH_3COO, ν SCN^- and $\nu ClO_4{}^-$, respectively. In the complex $[Mn(GBOA)_2(H_2O)_2]{\cdot}(CH_3COO)_2{\cdot}H_2O$, a band is observed at 1419 cm^{-1} assigned to ($\nu_{s(COO)}$). Such a band has been reported for ionic acetate [16b]. The ($\nu_{a(COO)}$) is not observed in the present case, as it merges with a strong broad band at 1544 cm^{-1} due to amide **II**($\nu_{C=N}$ amide). It is for this reason that $\nu_{a(COO)}$ band is not being reported for this complex. Further it has been reported that N-bound thiocyanate shows a band in the region of 2060–2080 cm^{-1}, while S-bound thiocyanate shows a band in the region of 2100–2115 cm^{-1} [16b]. In the present $[Mn(GBOA)_2(SCN)]\,(SCN){\cdot}4H_2O$ complex a strong band is observed at 2074 cm^{-1} confirming the presence of N-bound thiocyanate. In the complex $[Mn(GBOA)_2(ClO_4)]\,(ClO_4){\cdot}2CH_3CN$, a broad band is observed at 1135 cm^{-1}. A blow up of this band shows that the band is split into peaks arising at 1135, 1108 and 1091. This region covers both ionic/coordinated perchlorate anion [16b]. To further confirm whether both the anions are coordinated in the thiocyante/perchlorate bound complexes, molar conductance were obtained in dry DMF. The values found were 71.5 and 108 Ω^{-1} cm^2 mole^{-1} and are in keeping with values for a 1:1 electrolyte [16c].

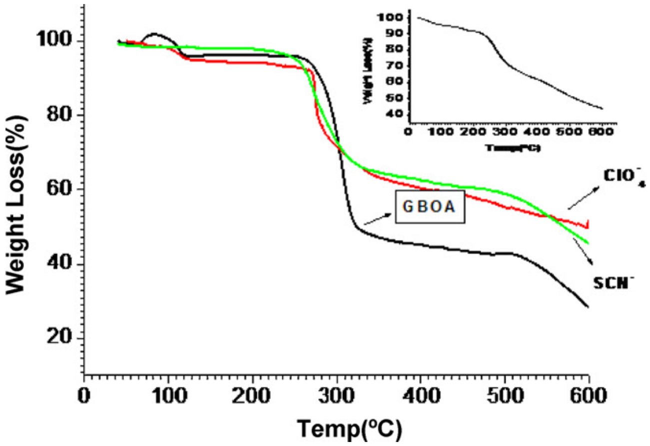

Fig. 1. TGA spectra of ligand (GBOA), $[Mn(GBOA)_2(SCN)]\,(SCN){\cdot}4H_2O$, $[Mn(GBOA)_2(ClO_4)]\,(ClO_4){\cdot}2CH_3CN{\cdot}0.5H_2O$ and $[Mn(GBOA)_2(H_2O)_2]{\cdot}(CH_3COO)_2{\cdot}H_2O$ (inserted figure).

Thermo grams of parent ligand GBOA and their respective Manganese(II) complexes are shown in Fig. 1. In the case of the free ligand GBOA, a major mass loss is observed in the temperature region 260–330 °C accounting for nearly 46.5% of the starting compound, while a mass loss of 4.6% is observed uptill 100 °C, confirming the presence of solvated water molecules.

For the complex $[Mn(GBOA)_2(H_2O)_2]{\cdot}(CH_3COO)_2{\cdot}H_2O$ a mass loss of about 5.5% is observed up to a temperature of 180 °C. The corresponding DTA shows two endothermic peaks in this temperature region confirming the loss of coordinated and solvated water molecules. Further a single mass loss of about 20% with one endothermic peak is found in the temperature regime 220–330 °C. This indicates the loss of ligand fragment and also the stability of the Mn(II) complex relative to the free ligand.

For the complexes $[Mn(GBOA)_2(SCN)]\,(SCN){\cdot}4H_2O$ and $[Mn(GBOA)_2(ClO_4)]\,(ClO_4){\cdot}2CH_3CN$ a loss of 4–5% is observed respectively, in the temperature range up to 120 °C implying loss of non coordinated water/solvent. While a mass loss of nearly 30% associated with two endothermic peaks, is observed in the temperature range 220–330 °C. This suggests loss of coordinated anion and ligand.

Thus the thermal studies show different mass loss behavior for the $[Mn(GBOA)_2(H_2O)_2]{\cdot}(CH_3COO)_2{\cdot}H_2O$ complex compared to the other two Mn(II) complexes strengthening the proposal of coordinated water in this complex.

3.2. EPR spectra

X-band solid state EPR spectra of the Mn(II) complexes were recorded at liquid nitrogen temperatures and are shown in Fig. 2. Spectra are spread over nearly 5000 gauss with several transition typical for a Mn(II) octahedral complex, undergoing weak tetragonal distortion [17(a,b)]. The main features are a strong transition at $g_{eff} = 2$ (3300–3400 G) and a relatively weak transition at $g_{eff} = 2.8$ (2400–2600 G). In the case of Mn(II) complex with $ClO_4{}^-$ as co-

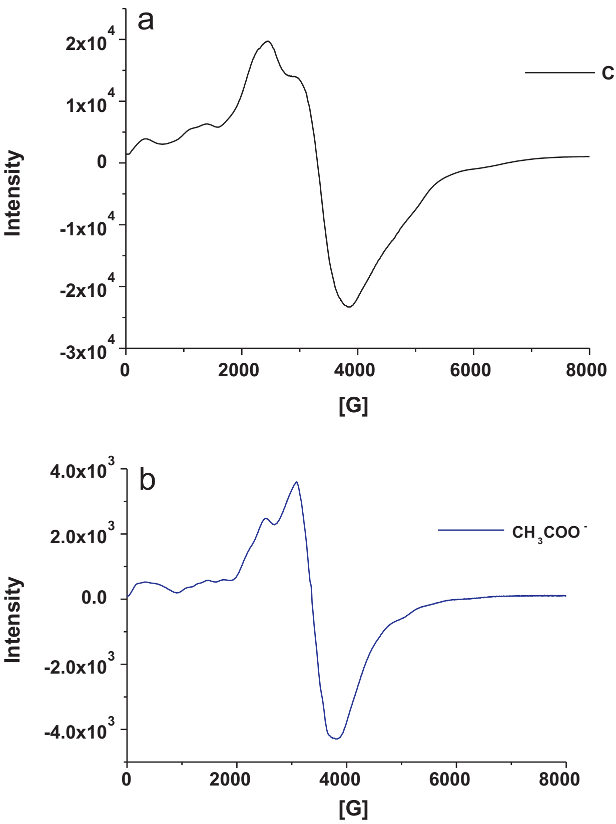

Fig. 2. (a) EPR spectra of $[Mn(GBOA)_2(H_2O)_2]\cdot(Cl)_2\cdot4H_2O$ in the solid state at microwave frequency 9.448 GHz and receiver gain 10^3. (b) EPR spectra of $[Mn(GBOA)_2(H_2O)_2]\cdot(CH_3COO)_2\cdot H_2O$ in the solid state at microwave frequency 9.448 GHz and receiver gain 10^3.

anion, a relatively strong $g_{eff} = 6$ (1100 G) is also observed, implying that this compound undergoes a larger axial distortion in comparison to others.

Zero field splitting parameter D (cm^{-1}) for the manganese complexes with $\lambda = 0.01$ has been obtained using the method of Dowsing et al. [17(c)] and the values compare well with other Mn(II) complexes undergoing weak axial distortion [17(d,e)]:

X	D (cm^{-1})
ClO_4^-	0.18
SCN^-	0.11
Cl^-, CH_3COO^-	0.05

The axial distortion for the complexes $MnLX_2$ decreases in the order $ClO_4^- > SCN^- > Cl^- \sim CH_3COO^-$. Thus the two complexes (1 and 2) where the anionic ligand is outside the coordination sphere and have coordinated water molecules have similar D parameter; this is also borne out from the similar resonance positions observed in their EPR spectra (Table 2). However it varies for the complexes (3 and 4) when the anionic ligand becomes part of the coordination sphere.

Table 2
Field position found in the EPR spectra of Diaquo-Mn(II) complexes.

Complexes	H_1(G)	H_2(G)	H_3(G)	H_4(G)	H_5(G)
$[Mn(GBOA)_2(H_2O)_2]\cdot(Cl)_2\cdot4H_2O$	400	1150	1470	2550	3000
$[Mn(GBOA)_2(H_2O)_2]\cdot(CH_3COO)_2\cdot H_2O$	400	1100	1500	2600	3100

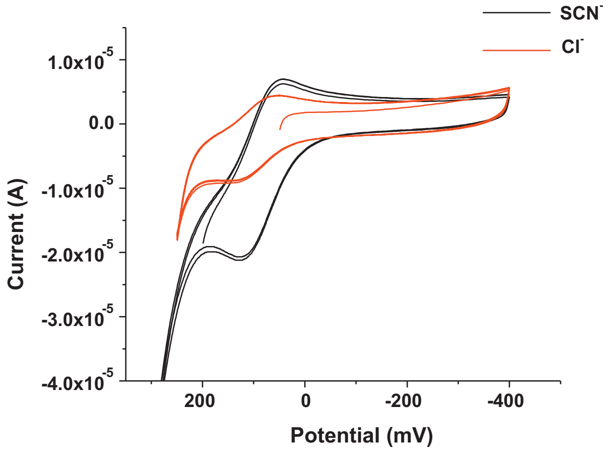

Fig. 3. Cyclic voltammogram spectra of $Mn(GBOA)_2(SCN)_2$ and $[Mn(GBOA)_2(H_2O)_2]\cdot(Cl)_2\cdot4H_2O$ in 2:8 (DMSO:AN).

3.3. Cyclic voltammetry

The cyclic voltammograms were recorded in 2:8 ($DMSO:CH_3CN$), containing 0.10 M TBAP as supporting electrolyte at a platinum working electrode. Ferrocene was used as internal standard and potentials are referenced to the Fc^+/Fc couple, shown in Fig. 3. The complexes display a quasi-reversible redox wave due to Mn(II)/Mn(III) process. The data reveals the instability of Manganese(II) oxidation state in the complexes, in the decreasing order $ClO_4^- > SCN^- > Cl \sim CH_3COO^-$ [$E_{1/2}$ vs Ag/Ag^+: 0.058, 0.080, 0.095, 0.097 (V)]. The pattern of $E_{1/2}$ values is related to the axial distortion parameter D obtained from EPR work. It is apparent that the $E_{1/2}$ becomes less anodic as the D value increases. The nearly similar value of $E_{1/2}$ for $[Mn(GBOA)_2(H_2O)_2]Cl_2\cdot4H_2O$ and $[Mn(GBOA)_2(H_2O)_2]\cdot(CH_3COO)_2\cdot H_2O$ further strengthens similar coordinating ligands.

3.4. Description of crystal structure

An ORTEP plot of the $[Mn(GBOA)_2(H_2O)_2](Cl)_2\cdot4H_2O$ (**1**) complex is depicted in Fig. 4. The coordination number around Mn^{2+} is six. Two trans coordination positions are occupied by two benzimidazole imine nitrogens N1 and N7 belonging to two different ligands, while the other two *trans* positions are occupied by amide oxygens O3 and O6; the remaining two positions are occupied by two oxygen atoms O1W and O2W belonging to water molecules. The two Cl^- anions are outside the coordination sphere. The asymmetric unit also contains four lattice water molecules labeled

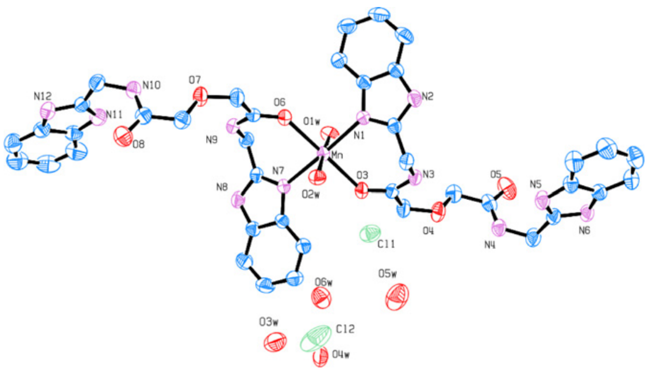

Fig. 4. Showing the ORTEP view of the molecule and the labeling scheme used in the structure analysis. Only the nitrogen and oxygen atoms have been labeled for the sake of clarity.

Table 3
Selected bond lengths and bond angles.

N1–Mn	2.223(2)
N7–Mn	2.223(2)
O1W–Mn	2.205(2)
O2W–Mn	2.202(2)
O3–Mn	2.183(2)
O6–Mn	2.184(2)
O3–Mn–O6	177.77(8)
O3–Mn–O2	91.18(8)
O6–Mn–O2	86.59(7)
O3–Mn–O1	85.69(8)
O6–Mn–O1	96.53(8)
O2–Mn–O1	176.10(7)
O3–Mn–N7	90.92(7)
O6–Mn–N7	89.10(7)
O2W–Mn–N7	90.20(8)
O1W–Mn–N7	87.52(8)
O3–Mn–N1	90.70(7)
O6–Mn–N1	89.43(7)
O2W–Mn–N1	93.71(8)
O1W–Mn–N1	88.67(8)
N7–Mn–N1	175.73(8)

O3W, O4W, O5W and O6W. The important bond lengths and bond angles are given in Table 3.

The coordination modes of the ligand are very unusual in the present complex. The ligand contains four potential coordination sites, two benzimidazole nitrogens, two amide oxygens. Earlier structural reports on this class of ligands reveals that this ligand is capable of forming mononuclear as well as dinuclear complexes with transition metal ions [11,15,16]. The size of the spacer between two amide groups appears to be the major factor determining the nature of complexation. If the chain length is long, then the ligand adopts a helical conformation and it wraps around the metal ion using all the four coordination sites to form a mononuclear complex [16]. If the chain length of spacer is small then the ligand adopts an extended conformation towards the metal ion and a dinuclear complex is formed. In both types of complexes all the four donor sites are used in complexation. It has also been observed that the two protonated benzimidazole nitrogens do not coordinate with the metal ion since under the reaction conditions these nitrogen atoms do not get deprotonated.

The present structure analysis reveals a new coordination mode of the ligand in which the ligand adopts an extended conformation and surprisingly only half the coordination sites are used for coordination to Mn^{2+}. The remaining benzimidazole nitrogen and the amide oxygen remain uncoordinated. Probably this is due to low CFSE in case of Mn^{2+} and extensive H-bonding observed in the structure. The two benzimidazole rings of each ligand are in gauche conformation with respect to each other (the dihedral angles between them being 59.44(6) and 69.00(7)°, respectively). Thus the coordinating rings have rotated inwards to facilitate coordination to the metal ion. The two coordinating and non-coordinating rings are parallel and *trans* to each other thus giving a 'S' like conformation to the molecule shown in Fig. 5, offering two 'U' shaped cavities per molecule.

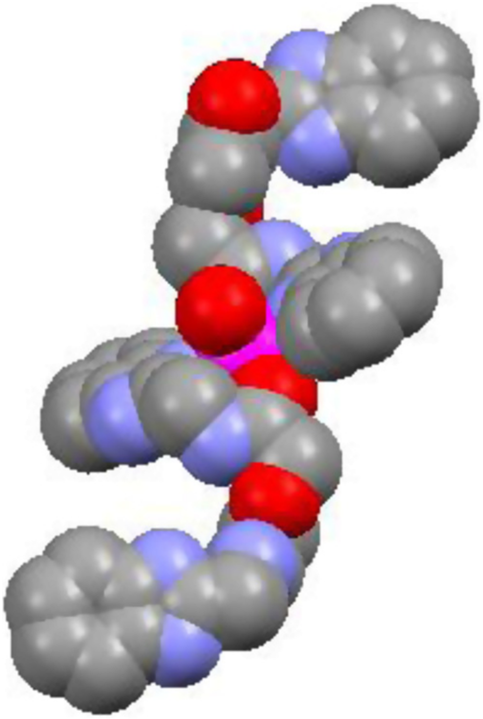

Fig. 5. Showing 'S' shaped conformation of the molecule.

3.4.1. H-bonding network

The crystal structure of the molecule is very interesting due to extensive H-bonding interactions involving coordinating and

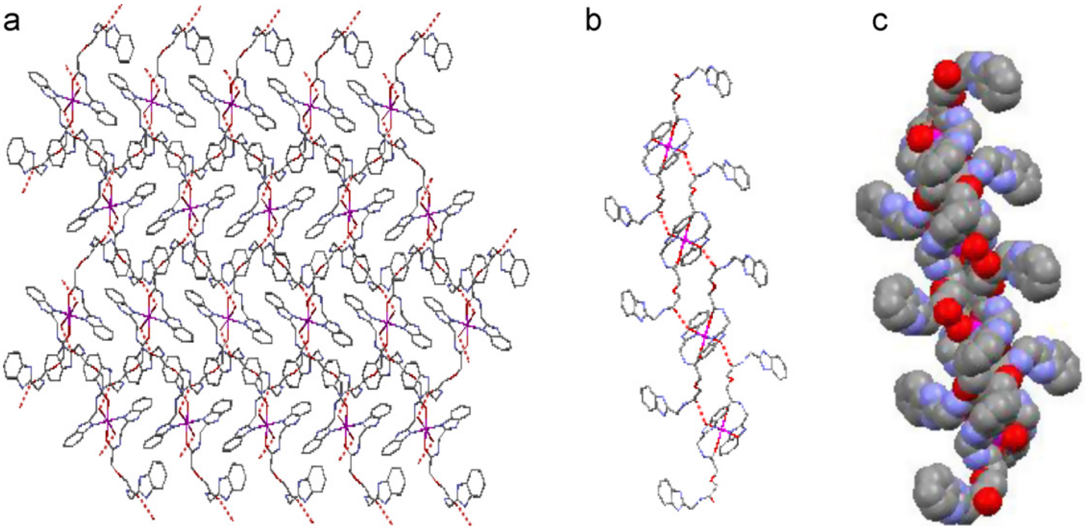

Fig. 6. Showing one of the helical sheets (a) in the *ab* plane, (b) in the *ac* plane (c) in the *ac* plane as space filling model; the hydrogens, lattice water molecules and chloride ions have been removed for clarity.

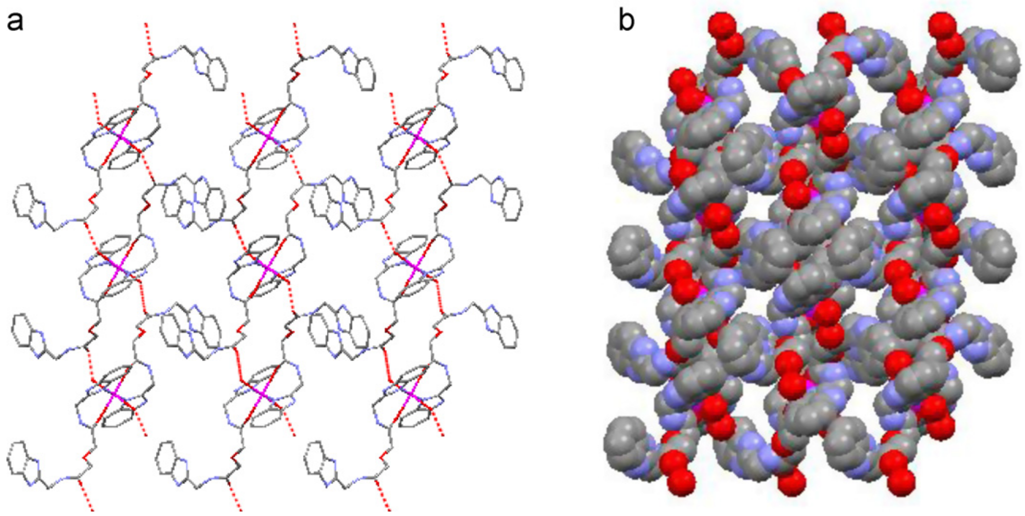

Fig. 7. Showing packing in the *ac* plane: (a) sheets arranged along *c* axis and (b) space filling model showing the solvent accessible voids.

lattice water molecules, nitrogens of the benzimidazole moiety, amide group and chloride ions. Table 3 contains a complete list of the H-bonding interactions whereas important ones of them have been shown in the various figures (*vide infra*). Crystal structure may be visualized considering the most important intermolecular H-bonding interactions between coordinating water molecules O1W and O2W and amide oxygens O5 and O8 respectively (Table 3) stabilizing the two uncoordinated amide oxygens. These two interactions form helical sheets of molecules in the *ab* plane as shown in Fig. 6. In these sheets the inward turned, coordinating benzimidazole rings are stabilized due to intermolecular $\pi\cdots\pi^*$ interactions between them (centroid to centroid distance 3.791(4) and 3.848(4) Å). At the same time the amide nitrogen N4 of the extended, non-coordinating part of the ligand, is forming H-bonds with the benzimidazole nitrogen N5 in these helical chains (not shown). The packing diagram of the molecule shows these sheets further extended along the *c* axis creating solvent accessible voids in them (Fig. 7).

These voids are filled with four water molecules and two Cl^- ions as shown in Fig. 8 which are involved in extensive H-bonding with the positively charged sheets and are holding them together, along the *c* axis. Fig. 9 illustrates the important H-bonding interactions among the guests (lattice water and Cl^- ions) and cationic layers. Cl1 anion is accepting H-bonds from coordinating water O2W and two lattice waters O5W and O6W as well as from two protonated imidazole nitrogens N6 and N12 whereas Cl2 anion is accepting four H-bonds from three lattice waters O3W, O5W and O6W and one imidazole nitrogen N8. At the same time the lattice waters O3W and O4W are also acting as H-bond donors to the amide nitrogens N10 and N4 and imidazole nitrogens N11 and N5, respectively. Both these water molecules are in turn receiving H-bonds from amide nitrogens N9 and N3, respectively. H-bonds between water molecules O4W and O6W and O1W and O5W gives rise to two dimeric water molecules. Some important references were found in the Cambridge Structure Database search for interactions in Mn(II) complexes having Cl^- ions and water molecules (both free and coordinating) and some N donor ligand molecules [18(a-d)]. These showed O(water)···Cl and N···Cl H-bonding interactions lying in the ranges 3.055–3.218 and 3.138–3.298 Å, respectively which are quite comparable to the values found in here (Table 4). They showed two to four H-bonding interactions with the Cl^- ion. In the present complex however, one of the Cl^- ions is involved in five such interactions. Thus this extensive H-bonding stabilizes the anions and at the same time reduces their nucleophilicity to an extent that a charge separated complex is formed.

In this context it may be pertinent to recall the role of chloride ions in the photosynthetic system, where it is proposed that Cl^- ions maintain a proton relay network that allows the transport and release of protons during the water oxidation reaction, and depletion of Cl^- ions causes a partial loss of water oxidase activity [8,19].

3.5. Amine binding and oxidation in the presence of tritert.butylhydroperoxide

A manganese dependant peroxidase (MnP) isozyme has been documented to oxidize aromatic amines [9]. Further ammonia and its analogues have been reported to bind to the Mn site on the water oxidase cluster [20] and more specifically to the S_2 state of the EPR active Mn-cluster in photosystem-II [21]. Earlier Mn tetraarylporphyrins have been utilized for the oxidation of primary aromatic amines to azo compounds using imidazole as co catalyst [21a], Shiffs base formation [21b] and oxidative coupling of

Table 4
Important H-bonding interactions (Å,°).

X–H···Y	X···Y	H···Y	∠X–H···Y
O2W–H22W···Cl1	3.206(2)	2.21	171
O3W–H32W···Cl2	3.139(2)	2.24	164
O5W–H51W···Cl2	3.387(3)	2.36	163
O5W–H52W···Cl1	3.250(3)	2.31	161
O6W–H61W···Cl2	2.945(3)	2.02	167
O6W–H62W···Cl1	3.206(3)	2.27	156
O4W–H42W···O6W	2.917(3)	2.01	158
N6–H61···Cl1^{I}	3.164(2)	2.18	168
N4–H41···N5^{I}	3.214(4)	2.29	151
N2–H21···O6W^{II}	2.839(3)	1.93	167
N3–H31···O4W^{II}	2.760(3)	1.91	147
O1W–H12W···O5W^{III}	2.814(3)	1.85	175
O2W–H21W···O8^{IV}	2.680(3)	1.74	178
N8–H81···Cl2^{V}	3.050(3)	2.15	174
N9–H91···O3W^{V}	2.802(3)	1.83	156
N10–H101···N11^{VI}	3.312(3)	2.43	150
N12–H121···Cl1^{VII}	3.245(2)	2.27	162
O1W–H11W···O5^{VIII}	2.789(3)	1.85	166
O3W–H31W···N10^{IX}	3.232(3)	2.82	102
O3W–H31W···N11^{IX}	2.825(3)	1.75	167
O4W–H41W···N5^{X}	2.786(3)	1.89	175
O4W–H41W···N4^{X}	3.495(3)	2.98	118

(I) $-x+1, -y, -z+1$ (II) $x, +y-1, +z$ (III) $x, -y+1/2, +z-1/2$. (IV) $-x+2, +y-1/2, -z+1/2$. (V) $x, -y+1/2+1, +z-1/2$. (VI) $-x+2, -y+1, -z$. (VII) $-x+2, +y+1/2, -z+1/2$. (VIII) $-x+1, +y+1/2, -z+1/2$. (IX) $x, -y+1/2+1, +z+1/2$. (X) $x, +y+1, +z$.

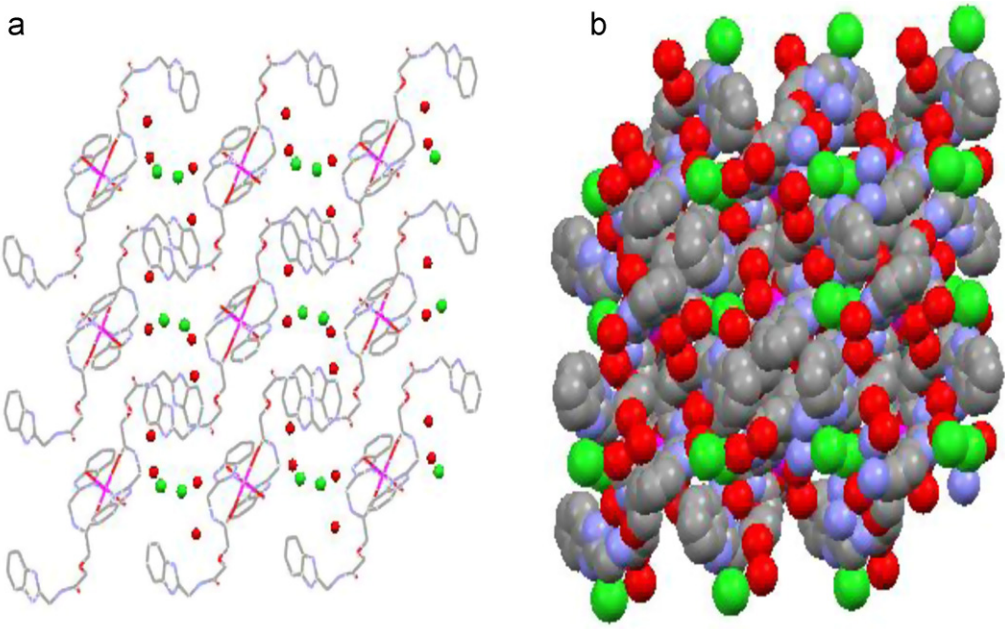

Fig. 8. Showing packing diagram in the *ac* plane: (a) the voids occupied by lattice water molecules (red) and Cl^- ions (green) and (b) the same as space filled models. (For interpretation of the references to color in this figure legend, the reader is referred to the web version of the article.)

amines to imines in the presence of oxidant Bu^tOOH [21c]. In view of these reports and since the basicity of tertiary amines is close to that of ammonia, we were prompted to study the reaction of tertiary amines with the present Mn(II) complex in the presence of an external oxidant i.e. tri-tert.butyl hydroperoxide as explained in the experimental section. It has been established earlier that, in the absence of protic solvent the hydroperoxides cleave by homolysis reaction [16a,22,23]. It is assumed that in the present case, similar reaction sequences are operative, wherein, the Manganese(II) catalyst promotes the homolysis of tri tert-butyl hydroxide, leading to the generation of tert butyl and hydroxyl radical. The tert butyl radical abstracts hydrogen atom from the benzylic (in the case of aromatic amines) or the aliphatic (in the case of pyrrolidone) methylene group, forming R_3COH and allowing the simultaneous attack of the $OH^\bullet$ on the electron deficient carbon atom resulting in the oxygenation of the substrate. This is depicted in the reaction Scheme 1. The percentage yield of the carbonyl products and the turnover of the Manganese(II) catalyst are given in Table 5.

Table 5
Product yields and turn over number.

Compound	Product	Complex (1)		Complex (2)	
		Yield (%)	Turn over	Yield (%)	Turn over
N-benzyldimethyl amine	Benzaldehyde	33.3	8[a]	30	7
Pyrollidine	Pyrollidinone	49.4	24	45	22

[a] The initial amount of N-benzyl dimethyl amine was 0.1505 mmol.

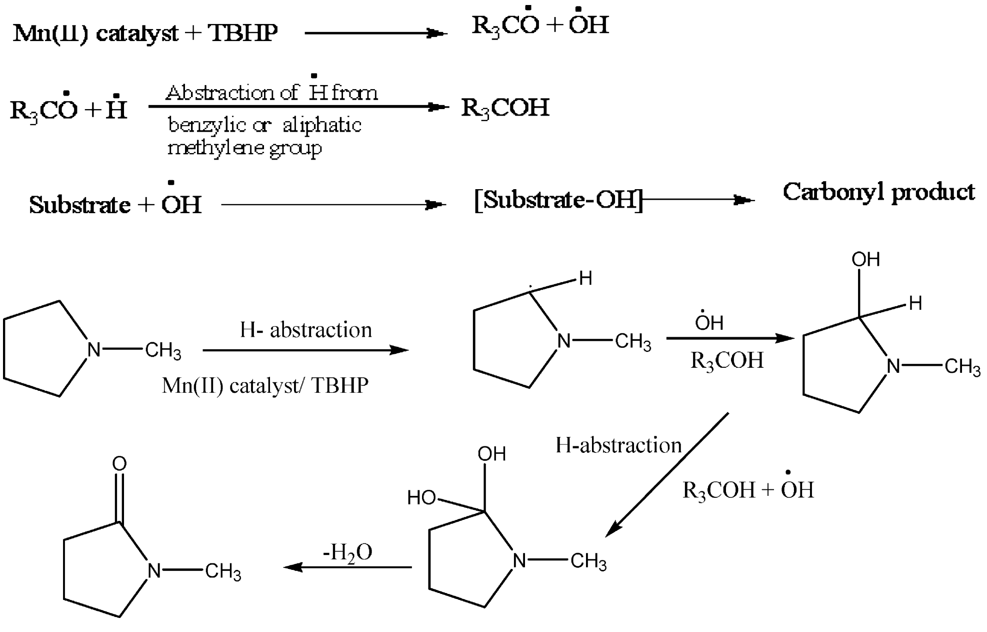

Scheme 1.

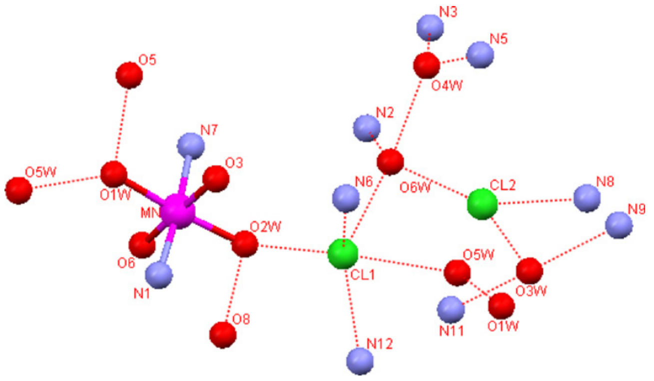

Fig. 9. Showing the H-bonding interactions around two anions Cl(1) and Cl(2) and the water molecules.

4. Conclusion

Four new Manganese(II) complexes with a bis-benzimidazolyl diamide ligand have been synthesized and one of them $[Mn(GBOA)_2(H_2O)_2]Cl_2{\cdot}4H_2O$ has been structurally characterized. In this complex the bis benzimidazolyl diamide ligand provides only two of the four potential binding sites to the Mn(II) ion leading to a stoichiometry of 1:2 for Mn:Ligand, respectively. The uncoordinated arms of the two ligands participate in intermolecular H-bonding leading to the formation of U-type cavities. The cavities host Cl^- anion and water molecules as guests. Two Cl anions remain uncoordinated to the Mn(II) ion but remain in the lattice. They participate in a uncommon $Cl\cdots HN$ and $Cl\cdots OH$ H-bonding mode resulting in a extended H-bonding network. Axial distortion parameter D has been obtained from EPR work for all the complexes and it is found to be dependant on whether the anionic ligand is in the coordination sphere or outside. Axial distortion for the Mn(II) complexes decreases in the order $ClO_4^- > SCN^- > Cl^- \sim CH_3COO^-$. Axial distortion D is smaller for complexes having two axial water molecules in the coordination sphere while the value is larger when the aquo ligand is replaced by an anionic ligand The complexes display a quasi-reversible redox wave due to Mn(II)/Mn(III) process. The data reveals the instability of Manganese(II) oxidation state in the complexes, in the decreasing order $ClO_4^- > SCN^- > Cl \sim CH_3COO^-$. $E_{1/2}$ values are found to be related to the D parameter found from EPR work, larger the D value less anodic the $E_{1/2}$. $[Mn(GBOA)_2(H_2O)_2]Cl_2{\cdot}4H_2O$ and $[Mn(GBOA)_2(H_2O)_2]{\cdot}(CH_3COO)_2{\cdot}H_2O$ carry out the selective oxidation of N-benzyldimethylamine, and 1-methyl-pyrollidine to their respective carbonyl products with catalytic efficiency of 35–50%.

The oxidation of amines by the complex along with the role of Cl anion in the formation of a extended H-bonding network is reminiscent of roles in a Mn(II) dependant peroxidase from lignin and the Manganese containing Oxygen evolving complex of Photosystem-II.

Acknowledgment

We gratefully acknowledge financial support from the Defence Research Development Organization, Directorate of Extramural Research and Intellectual Property Rights, India, and to Prof. U.P. Singh, Department of Chemistry, IIT Roorkee, Roorkee, India for collecting the X-ray diffraction data.

Appendix A. Supplementary data

Supplementary data associated with this article can be found, in the online version, at doi:10.1016/j.saa.2011.05.024.

References

[1] J.M. Lehn, Supramolecular Chemistry, VCH, Weinheim, 1995.
[2] D. Braga, F. Grepioni, G.R. Desiraju, Chem. Rev. 98 (1998) 1375–1406.
[3] H.J. Choi, T.S. Lee, M.P. Suh, Angew. Chem. Int. Ed. 38 (1999) 1405–1408.
[4] C.S. Liu, X.S. Shi, J.R. Li, J.J. Wang, X.H. Bu, Cryst. Growth Des. 6 (2006) 656–663.
[5] J.M. Lehn, Angew. Chem. Int. Ed. Engl. 29 (1990) 1304–1319.
[6] B. Moulton, M.J. Zaworotko, Chem. Rev. 101 (2001) 1629–1658.
[7] S. Changyan, Z. Xiangjun, J. Linpei, J. Mol. Struct. 646 (2003) 201–210.
[8] S. Mukhopadhyay, S.K. Mandal, S. Bhaduri, W.H. Armstrong, Chem. Rev. 104 (2004) 3981–4026.
[9] H. Wariishi, K. Valli, M.H. Gold, J. Biol. Chem. 267 (1992) 23688–23695.
[10] L.A. Cescon, A.R. Day, J. Org. Chem. 27 (1962) 581–586.
[11] M. Gupta, S.K. Das, P. Mathur, A.W. Cordes, Inorg. Chim. Acta 353 (2003) 197–205.
[12] A. Altomare, M.C. Burla, M. Camalli, G.L. Cascarano, C. Giacovazzo, A. Guagliardi, A.G.G. Moliterni, G. Polidori, R. Spagna, J. Appl. Cryst. 32 (1999) 115–119.
[13] G.M. Sheldrick, Programs for Crystal Structure Analysis (Release 97-2) Institüt für Anorganische Chemie der Universität, Tammanstrasse 4, D-3400 Gottingen, Germany, 1998.
[14] L.J. Farrugia, J. Appl. Cryst. 32 (1999) 837–838.
[15] S.C. Mohapatra, S. Tehlan, M.S. Hundal, P. Mathur, Inorg. Chim. Acta 361 (2008) 1897–1907.
[16] (a) S. Tehlan, M.S. Hundal, P. Mathur, Inorg. Chem. 43 (2004) 6589–6595;
(b) K. Nakamoto, Infrared and Raman Spectra of Inorganic and Coordination compounds, 5th edition, Wiley, New York, 1997;
(c) W.J. Geary, Coord. Chem. Rev. (1971) 122–781.
[17] (a) M. Singla, P. Mathur, Spectrochim. Acta Part A 74 (2009) 536–543;
(b) S.J. Brudenell, L. Spiccia, A.M. Bond, G.D. Fallon, D.C.R. Hockless, G. Lazarev, P.J. Mahon, E.R.T. Tiekink, Inorg. Chem. (2000) 39881–39892;
(c) R.D. Dowsing, J.F. Gibson, M. Goodgame, P.J. Hayward, J. Chem. Soc. (A) (1969) 187–193;
(d) P. Mathur, M. Crowder, G.C. Dismukes, J. Am. Chem. Soc. 109 (1987) 5227–5233;
(e) C. Hureau, L. Sabater, E.A. Mallart, M. Nierlich, M.F. Charlot, F. Gonnet, E. Riviere, G. Blond, Chem. Eur. J. 10 (2004) 1998–2010.
[18] (a) T.O. Vardosanidze, V.I. Sokol, A.N. Sobolev, A.E. Shvelashvili, M.A. Porai-Koshits, Russ. J. Inorg. Chem. 30 (1985) 1745–1751;
(b) S. Wang, T.D. Westmoreland, Inorg. Chem. 48 (2009) 719–727;
(c) P. Bonhote, M. Ferigo, H. Stoeckli-Evans, W. Marty, Acta Cryst. C 49 (1993) 2102–2107;
(d) B.B. Levaton, M.M. Olmstead, Acta Cryst. E 66 (2010) m1226–m1227.
[19] K. Olesen, L.-E. Andreasson, Biochemistry 42 (2003) 2025–2035.
[20] P.O. Sandusky, C.F. Yocum, Biochim. Biophys. Acta 766 (1984) 603–611.
[21] (a) F.B. Warren, C. de Paula Julio, W.B. Gary, J. Am. Chem. Soc. 108 (1986) 4018–4022;
(b) A. Rezaeifard, M. Jafarpour, S. Rayati, R. Shariati, Dyes Pigments 80 (2009) 80–85;
(c) S. Tollari, A. Fumagalli, F. Porta, Inorg. Chim. Acta 247 (1996) 71–74;
(d) Q. Lan Yuan, X. Tai Zhou, H. Bing Ji, Catal. Commun. 12 (2010) 202–206.
[22] D. Chin, G.N. Mar La, A.L. Balch, J. Am. Chem. Soc. 120 (1980) 5945–5947.
[23] R.D. Arasasingham, A.L. Balch, L. Latos-Grazynski, J. Am. Chem. Soc. 109 (1987) 5846.